

Original Article

Adsorption of ibuprofen compounds using magnetic molecularly imprinted polymers

Halimah Fahri*, Muhammad Ali Zulfikar, and Muhammad Yudhistira Azis

*Department of Chemistry, Faculty of Mathematics and Natural Sciences,
Bandung Institute of Technology, Bandung, Jawa Barat, 40132 Indonesia*

Received: 13 July 2023; Revised: 26 October 2023; Accepted: 16 November 2023

Abstract

Ibuprofen (IBP) is commonly found in aquatic environments originating from pharmaceutical waste and the metabolic results of humans who consume it. To remove IBP, an adsorption method was used with magnetic molecularly imprinted polymer (MMIPs) as an adsorbent synthesized by bulk polymerization of ibuprofen (IBP) as a template, methacrylic acid (MAA) as a monomer, and divinylbenzene (DVB) as a crosslinker, in the molar ratio 1:4:20 in acetonitrile porogen. Fe₃O₄ nanoparticles and MMIPs were characterized by Fourier Transform Infrared Spectroscopy (FTIR), Scanning Electron Microscope-Energy Dispersive Spectroscopy (SEM-EDS), Transmission Electron Microscopy (TEM), Vibrating Sample Magnetometer (VSM), and Zeta Potential Analyzer. IBP removal was near optimal from a batch at pH 3 with a contact time of 90 minutes and an adsorbent mass of 25 mg. The IBP adsorption process followed a pseudo-second-order adsorption kinetics model, and the Langmuir isotherm adsorption with a maximum adsorption capacity of 151.37 mg/g took place spontaneously and was exothermic.

Keywords: ibuprofen, adsorption, magnetic, polymer

1. Introduction

Ibuprofen (IBP) is an acidic pharmaceutical that belongs to the class of non-steroidal anti-inflammatory drugs (NSAIDs), which is most widely used to treat inflammation and as an analgesic, antipyretic, and antirheumatic (Madikizela & Chimuka, 2016; Samah, Sánchez-Martín, Sebastián, Valiente, & López-Mesas, 2018). The high level of consumption of this compound causes ibuprofen to be detected in the environment due to direct discharge into aquatic systems and incomplete removal during wastewater treatment. Wastewater treatment plants (WWTP) find high concentrations of these drugs in human urine or fecal excretion, and in pharmaceutical manufacturing discharges (Farré *et al.*, 2001). The presence of these compounds in water can cause serious risks to the environment and human health because they can cause genotoxicity, aquatic toxicity, and resistance development in pathogenic bacteria (Moral-Rodríguez, Leyva-Ramos, Carrasco-Marín, Bautista-Toledo,

& Pérez-Cadenas, 2020). Several techniques are used to remove IBP, including filtration, electrocoagulation, ozonation, photocatalysis, and adsorption (AL Falahi *et al.*, 2021; Sahin, Saygi-Yalcin, & Saloglu, 2020). However, the implementations of these techniques are only partly efficient because of being limited to removing organic compounds, and toxicological oxidation by-products may be formed during the treatment processes that can exacerbate environmental and human health impacts (Dai, Geissen, Zhang, Zhang, & Zhou, 2011). Adsorption is the most popular technique for removing organic contaminants such as pharmaceuticals because it is very effective, simple, relatively inexpensive, and does not cause secondary water pollution (Lach & Szymonik, 2020). Several of the adsorbents that have been used to adsorb IBP are porous adsorbents, such as clay and minerals, activated clay, activated carbon, graphene oxide, and so on (Oba, Ighalo, Aniagor, & Igwegbe, 2021). However, all of these adsorbents have relatively low selectivity (Dai *et al.*, 2011).

Molecularly imprinted polymers (MIPs) are one type of adsorbents that have a high level of target selectivity (Fauziah, Soekamto, Budi, & Taba, 2019). MIPs are synthesized by the polymerization of functional monomers and crosslinkers in the presence of a template molecule. Then,

*Corresponding author

Email address: halimahlily5@gmail.com

when the template molecule is released, it will leave a cavity that is used to bind the target molecule (Husin *et al.*, 2021). MIPs have advantages including high selectivity, easy preparation, low cost, reusability, and high stability (Xia, Yun, Li, Huang, & Liang, 2017; Zhi *et al.*, 2018). However, MIPs are difficult to separate from the solution, but they can be modified with magnetite particles (MMIPs) to facilitate separation using an external magnet (Uzuriaga-Sánchez *et al.*, 2017). In addition, MMIPs have advantages such as fast binding and separation due to the magnetic properties; and have a uniform shape so that the polymer does not need to be ground (Rizqi, Zulfikar, & Wahyuningrum, 2021).

In this work, IBP adsorption is assessed using magnetic molecularly imprinted polymers (MMIPs) synthesized with ibuprofen (IBP) as a template, methacrylic acid (MAA) as a functional monomer, divinylbenzene (DVB) as a crosslinker, benzoyl peroxide (BPO) as an initiator and acetonitrile as a porogen. The adsorption performance of MMIPs was evaluated by parameters of solution pH, interaction time, adsorbent mass, adsorption isotherms, kinetics, and thermodynamic studies.

2. Materials and Methods

2.1 Materials

The materials used in this work include ibuprofen (IBP, Aldrich), naproxen (NPX, Aldrich), methacrylic acid (MAA, Aldrich), divinylbenzene (DVB, Aldrich), benzoyl peroxide (BPO, Merck), polyvinyl pyrrolidone (PVP, Aldrich), FeSO₄·7H₂O (Merck), FeCl₃·6H₂O (Merck), NH₄OH (Merck), oleic acid (Merck), acetonitrile (Merck), HPLC-grade methanol (Merck), and distilled water.

2.2 Synthesis of Fe₃O₄ nanoparticles

Fe₃O₄ nanoparticles were synthesized by the co-precipitation method (Rizqi Utami *et al.*, 2021). 0.6950 g of FeSO₄·7H₂O and 1.3515 g FeCl₃·6H₂O were dissolved in 100 mL distilled water and stirred until homogeneous at 80°C. Subsequently, NH₄OH was added dropwise to the above solution with vigorous mechanical stirring until a black precipitate (pH 9) was formed. The solution was stirred for 15 min then 2 mL of oleic acid was added, and the mixture was stirred for 15 min. The synthetic Fe₃O₄ nanoparticles were separated, washed with distilled water and ethanol several times and then separated from the solution using an external magnetic field. Then the magnetite Fe₃O₄ nanoparticles were dried in an oven at 60°C.

2.3 Synthesis of magnetic molecularly imprinted polymers (MMIPs)

MMIPs were prepared by bulk polymerization (He *et al.*, 2014; Huang *et al.*, 2012). 1 mmol of ibuprofen and 4 mmol of methacrylic acid in 10 mL acetonitrile were stirred to prepare the pre-polymerization solution. Subsequently, 20 mmol of DVB and 1 g Fe₃O₄ were added to the above solution. Then the PVP solution was added to the pre-polymerization solution. After that, 150 mg of BPO was added to the solution while flowing nitrogen gas for 5 minutes

to remove dissolved oxygen in the solution. Polymerization took place in an oil bath at 70°C with continuous stirring for 3 hours. The MMIPs precipitate that formed was separated from the solution using an external magnetic field and washed several times with acetonitrile. The template was removed by washing the MMIPs with acetonitrile solution several times until IBP was not detected and the MMIPs were dried in the oven at 60°C. The magnetic non-molecularly imprinted polymers (MNIPs) were synthesized under the same conditions, except that no template molecules were added in the polymerization process.

2.4 Material characterizations

The functional groups were identified using FT-IR Prestige-21 (Shimadzu, Japan) with a KBr pellet type sample, over the wavenumber range 4000-450 cm⁻¹. A scanning electron microscope with energy dispersive spectroscopy (JEOL JSM-6510 LA) and a transmission electron microscope (Hitachi HT7700, Japan) were used to observe the surface morphology of materials and to determine the element contents in materials. Vibrating sample magnetometer (VSM-250) was used to measure the magnetic properties of the samples at room temperature. Zeta potential analyzer (HORIBA SZ-100) was used to measure the zeta potential over the pH range 2-8. Analysis of adsorption was done using a UV-Vis Spectrophotometer at a wavelength of 222 nm.

2.5 Batch adsorption experiments

To investigate the adsorption capacity of the polymer, the effects of the experimental parameters namely pH (2–8), contact time (10–150 min), and adsorbent dose (10–30 mg) on the IBP removal were studied in batch mode. The stock solution was prepared by dissolving the accurate amount of IBP (99%) in methanol and distilled water solutions (1:1, v:v), and the working solutions were made up by dilution. In adsorption isotherm and thermodynamic studies, 25 mg MMIPs were added to 25 mL of IBP solution with the initial concentrations ranging from 40 to 300 mg/L. The solutions were placed for 90 min at 298, 313, and 333 K to reach adsorption equilibria, respectively. After 90 min, the MMIPs were isolated by an external magnetic field. In the study of adsorption kinetics, 25 mL solution with the initial IBP concentration of 50 mg/L was reacted with 25 mg of adsorbent in a batch experiment for various contact times (10–150 min), and the residual amount of IBP in the solution was measured using a UV/Vis spectrophotometer at 222 nm. The removal percentage and adsorption capacity of adsorbed IBP into MMIPs were calculated as follows:

$$q_e = \frac{(C_i - C_e)V}{m} \quad (1)$$

$$\% \text{Removal} = \frac{(C_i - C_e)}{C_i} \times 100\% \quad (2)$$

where q_e is the adsorption capacity (mg/g), C_i is the initial concentration of IBP (mg/L), C_e is the equilibrium concentration of IBP (mg/L), V is the volume of solution (L) and m is the sorbent mass (g).

3. Results and Discussion

3.1 Materials characterization

3.1.1 FTIR analysis

The FTIR spectra of Fe₃O₄, MNIPs, MMIPs before leaching, MMIPs after leaching, and MMIPs after adsorption are illustrated in Figure 1. The presence of Fe₃O₄-oleic acid is confirmed by the absorption band at 582 cm⁻¹, which was attributed to the Fe-O stretching vibrations. A broad band at 3,427 cm⁻¹ is ascribed to the O-H stretching vibrations on the surface of Fe₃O₄ which binds to oleic acid, and the hydrogen bonds between MAA and IBP. The peaks around the wavenumber of 2,922 cm⁻¹ were ascribed to the C-H stretching vibrations of oleic acid and other constituents of MMIPs and MNIPs. The peaks at 1,708 cm⁻¹ and 1,107 cm⁻¹ in the spectra (b), (c), and (d) show vibrations of the C=O and C-O bonds of methacrylic acid and IBP.

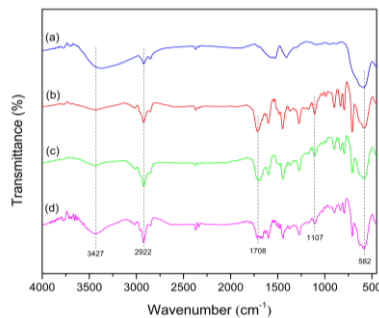


Figure 1. FTIR spectra of (a) Fe₃O₄, (b) MNIPs, (c) MMIPs before leaching, and (d) MMIPs after leaching

3.1.2 SEM-EDS and TEM analysis

The morphology of Fe₃O₄ nanoparticles, MNIPs, MMIPs before leaching, and MMIPs after leaching were observed by SEM-EDS and TEM, shown in Figure 2. Based on Figure 2 (a), the Fe₃O₄ nanoparticles appear to be agglomerated, demonstrating a tendency to interact with each other due to their magnetic properties. Observed in Figure 2. (b), (c) and (d) are the morphologies of MNIPs, MMIPs before leaching, and MMIPs after leaching. The spherical particles had a regular shape, a uniform size, and had specific

cavities (Olcer *et al.*, 2017). This is because in the synthesis method the polymer is modified with Fe₃O₄ nanoparticles which act as the core of the polymer. After removing the IBP template molecules from the polymer, the MMIPs surface morphology was spherical. This is due to the loss of various impurities and unreacted constituent compounds. The contents of C, O, and Fe in the materials were determined using an EDS, and the results are presented in Table 1. TEM analysis was also carried out to support the results from SEM analysis and the TEM images of Fe₃O₄ nanoparticles and MMIPs after leaching are shown in Figure 2 (e) and (f).

In Figure 2 (e) and (f), the morphology of Fe₃O₄ nanoparticles can be observed and the Fe₃O₄ nanoparticles exhibit slight agglomeration. This agglomeration occurs due to the tendency of Fe₃O₄ nanoparticles to aggregate through Van der Waals forces, which are influenced by their magnetic properties. On the other hand, the TEM image of the MMIPs after leaching exhibits the spherical structure with a uniform diameter measuring 423 nm. This result is supported by a study conducted by Olcer, Demirkurt, Demir, & Eroglu, 2017, which also showed that the synthesized polymer produced a spherical morphology, although that polymer was not modified with magnetic nanoparticles.

Table 1 shows that Fe₃O₄ nanoparticles contain carbon atoms that come from coating the surface of Fe₃O₄ nanoparticles with oleic acid to prevent agglomeration. The amount of carbon elements for MNIPs, MMIPs before leaching, and MMIPs after leaching is the most dominant because all the constituent components of the polymer have carbon atoms. Apart from that, there was a decrease in the presence of oxygen and iron atoms for MMIP after leaching because the leaching process causes Fe₃O₄ nanoparticles to be released from the polymer. However, with this small composition, they were able to give good magnetic properties to the polymer that had been made.

Table 1. Data of element analysis of Fe₃O₄ nanoparticles, MNIPs, MMIPs before leaching, and MMIPs after leaching

Sample	Element content		
	C %	O %	Fe %
Fe ₃ O ₄ nanoparticles	24.67	48.04	27.29
MNIPs	90.48	7.77	1.74
MMIPs before leaching	82.91	13.84	3.25
MMIP after leaching	94.30	5.23	0.47

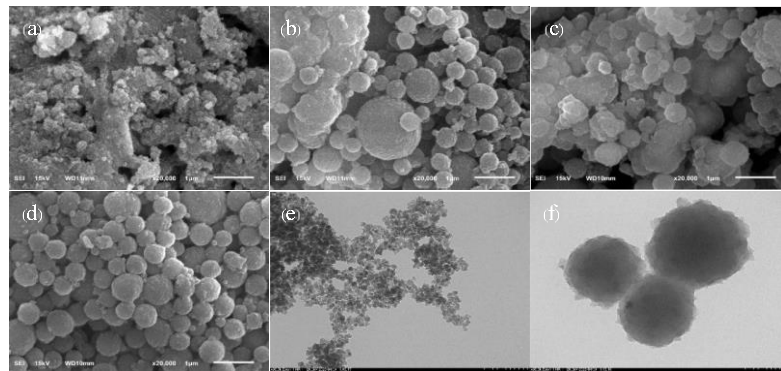


Figure 2. SEM images of (a) Fe₃O₄ nanoparticles, (b) MNIPs, (c) MMIPs before leaching, (d) MMIPs after leaching, TEM images of (e) Fe₃O₄ nanoparticles and (f) MMIPs after leaching at 30,000× magnification

3.1.3 VSM analysis

The magnetic properties of Fe₃O₄ nanoparticles and MMIPs were evaluated using a vibrating sample magnetometer (VSM) at room temperature. The magnetization saturation values (M_s) of Fe₃O₄ nanoparticles and MMIPs were found to be 48.81 emu/g and 14.87 emu/g, respectively, as shown in Figure 3. The decrease in magnetization of MMIPs could be attributed to the coating of a polymeric layer on the surface of the Fe₃O₄ nanoparticles. However, despite the decrease in M_s , the magnetic force exhibited by MMIPs was still sufficiently strong to effectively separate IBP from the solution. The coercivity values (H_c) of Fe₃O₄ nanoparticles and MMIPs after leaching were measured to be 81.22 Oe and 86.39 Oe respectively, indicates they have soft magnetic properties (Yulianti & Darvina, 2020).

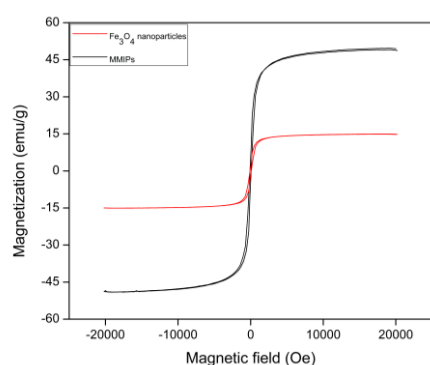


Figure 3. Hysteresis loop of Fe₃O₄ nanoparticles and MMIPs after leaching

3.2 Adsorption activity studies

3.2.1 Effect of pH

The effect of pH on IBP adsorption was studied in the pH range (2–8), by adjusting the solutions to the desired levels using HCl or NaOH. The effect of pH on 25 mg MMIPs with IBP 50 mg/L during a 90 min contact time is shown in Figure 4 (a). The optimal adsorption capacity is obtained at pH 3. At pH 2 to 3, there is an increase in adsorption capacity because the adsorbent surface which is positively charged will interact electrostatically with the –OH group which is charged negatively on IBP, but then the adsorption capacity decreases with further increase in pH because IBP has a pKa of 5.2

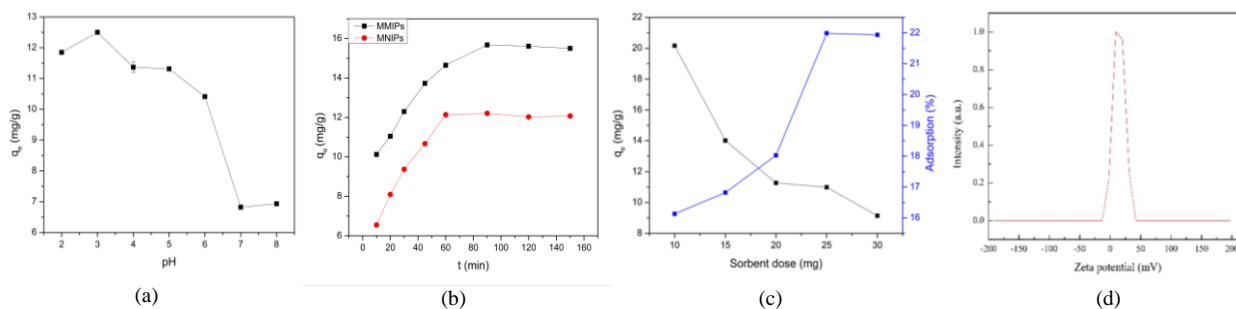


Figure 4. Effects of (a) pH, (b) contact time, and (c) sorbent dose on adsorption of IBP by MMIPs; and (d) zeta potential curve.

(Ningtyas, Zulfikar, Piluharto, 2015), which means that IBP will be negatively charged at pH above 5.2. An increase in pH causes the functional groups, both in the cavity and on the surface of the MMIPs to deprotonate, which results in negatively charged MMIP adsorbent so that there is no electrostatic attraction between the adsorbent and IBP because there is a repulsive force between negative charges and the cavity or active side available for absorption also becomes less (Olcer *et al.*, 2017). This result is also supported by the zeta potential analysis shown in Figure 4 (d), where the zeta potential for the MMIPs adsorbent at pH 3 is positive (14.4 mV), indicating that attractive electrostatic interactions occur between the surface of the MMIPs adsorbent and the anionic IBP analyte (Sahin *et al.*, 2020).

3.2.2 Effect of contact time

The effect of the contact time on adsorption capacity of MMIPs for IBP was investigated with various contact times (10-150 min). The effect of contact time with 25 mg of MMIP and IBP 50 mg/l at pH 3 is shown in Figure 4 (b). The adsorbed amount of IBP gradually increased as the contact time was prolonged until reaching an equilibrium. The optimal adsorption capacity was obtained at 90 min for MMIPs and 60 min for MNIPs. This is because increasing the contact time will increase the affinity of the active site on sorbent surfaces with the analyte. Afterwards, adsorption capacity obtained tends to be constant because the surface of the sorbent is saturated with adsorbate, which means that there is no active sites left on the surface of the sorbent to interact with the adsorbate.

3.2.3 Effect of sorbent dose

In order to evaluate the optimum MMIPs dose for the IBP adsorption, experiments were carried out in solutions of 50 mg/L at pH 3 for a duration of 90 min. Different amounts of the sorbent were added within the range of 10-30 mg. Figure 4 (c) illustrates the effect of the sorbent dose on the adsorption process. It is observed that increasing the mass of the sorbent leads to an increase in the adsorption efficiency and a decrease in adsorption capacity. This is because an increase in the number of sorbents will increase the number of active sites so the adsorption efficiency will increase, but these active sites will compete with each other for adsorption of adsorbate will thus cause adsorption capacity decrease if compared to a small amount of adsorbent (Rizki, Syahputra, Pandia, & Halimatuddahlia, 2019). The optimal sorbent

dose was determined to be 25 mg, beyond which the adsorption percentage reached a constant. This indicates that all the active sites on the sorbent surface have been occupied by the adsorbate, resulting in a saturation of the adsorption process. The number of active sites is proportional to the area of sorbent surface and each active site can only adsorb one adsorbate molecule. In a situation where the adsorption site is saturated by adsorbate, a sorbent concentration increase tends not to increase the amount of the substance adsorbed (Rizki *et al.*, 2019).

3.2.4 Adsorption isotherms

The binding properties and the equilibrium adsorption of MMIPs for IBP were studied by fitting to the Langmuir and Freundlich isotherm models as shown in Figure 6. Langmuir model, described by equation (3), is commonly used to characterize monolayer adsorption and homogeneous adsorption. This model assumes that the adsorbent surface is uniform and that the adsorption energy is constant throughout. Additionally, the Langmuir model assumes that each active site on the adsorbent can only be occupied by one molecule, and there is no interaction between the adsorbed molecules (Zhang *et al.*, 2021). The Freundlich model, described by equation (4), is an empirical equation that can be applied to adsorption on both heterogeneous surfaces and multilayer adsorption (Zhang *et al.*, 2021). This model introduces a heterogeneity factor, $1/n$, which characterizes the surface heterogeneity (Zulfikar, Wahyuningrum, Mukti, & Setiyanto, 2015). The non-linear forms of the Langmuir and Freundlich isotherm models (Zhang *et al.*, 2021) are as follows:

$$q_e = \frac{K_L q_{max} C_e}{1 + K_L C_e} \tag{3}$$

$$q_e = K_F C_e^{1/n} \tag{4}$$

where q_e (mg/g) is the amount of IBP adsorbed at equilibrium, C_e (mg/L) is the equilibrium concentration of IBP, K_L is the Langmuir binding constant which is related to the energy of adsorption, q_{max} (mg/g) is the maximum adsorption capacity of IBP, K_F is Freundlich constants related to adsorption capacity, and the $1/n$ is a measure of exchange intensity or surface heterogeneity, with a value of $1/n$ smaller than 1.0 describing a favorable removal condition. All of the constants were calculated by fitting the equations (Zhang *et al.*, 2021).

As seen in Figure 6 that shows the curve fits to the experimental data, the adsorption capacity increased with the concentration of IBP. The parameters of the two isotherms calculated based on Equations (3) and (4) by non-linear regression are presented in Table 2. Based on the results presented in Figure 6, it can be observed that the Langmuir isotherm provides a better fit to the experimental data than the Freundlich isotherm. This suggests that the adsorption of IBP onto the MMIPs follows a monolayer adsorption mechanism. Furthermore, the isotherm parameters obtained from the Langmuir model exhibit a higher regression coefficient, indicating a better-fitting result. The maximum adsorption capacity of IBP onto the MMIPs at pH 3 and 25°C, as determined by the Langmuir isotherm model, is found to be 151.37 mg/g. These findings highlight the effectiveness of the Langmuir isotherm model in describing the adsorption behavior of IBP onto the MMIPs.

Table 2. Isotherm parameters for adsorption of IBP on MMIPs.

Langmuir			Freundlich		
q_{max} (mg/g)	K_L (L/mg)	R^2	K_f (L/mg)	n	R^2
151.37	0.0019	0.9963	0.6679	1.2812	0.9867

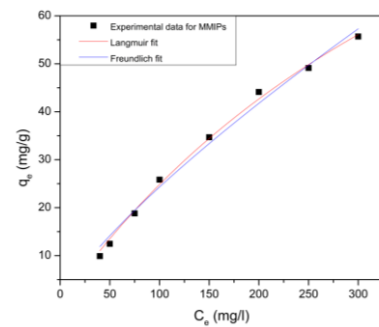


Figure 5. Non-linear fits by Langmuir and Freundlich isotherms to IBP adsorption by MMIPs

3.2.5 Adsorption kinetics

In this kinetics study, adsorption rates and equilibrium constants of pollutant adsorption were assessed. In this study, pseudo-first-order and pseudo-second-order

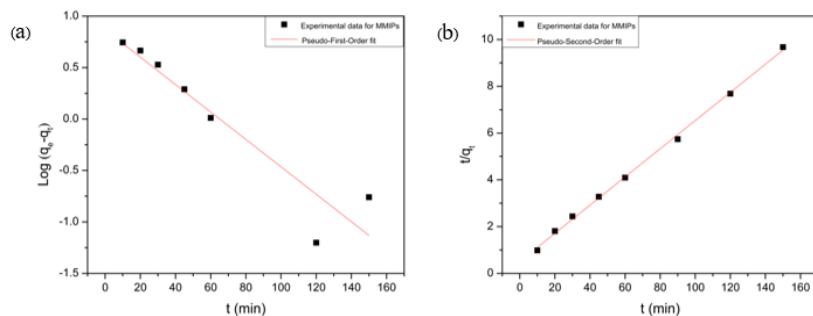


Figure 6. Linear fits by (a) pseudo-first-order, and (b) pseudo-second-order kinetics to adsorption of IBP by MMIPs

kinetic models were used to investigate the mechanism of adsorption of IBP onto MMIPs. The results shown in Figure 6 (a) and (b) were obtained at an initial concentration of 50 mg/L and a temperature of 25°C. The equilibration time needed for the adsorption of IBP was approximately 90 min for MMIPs. The pseudo-first-order and pseudo-second-order kinetic models, presented by equations (5) and (6) respectively (Zulfikar *et al.*, 2015), are as follows:

$$\text{Log}(q_e - q_t) = \log q_e - \frac{k_1 t}{2,303} \quad (5)$$

$$\frac{t}{q_t} = \frac{1}{k_2 q_e^2} + \frac{t}{q_e} \quad (6)$$

where q_t is the amount of adsorption of IBP (mg/g) at time t (min), and k_1 (min^{-1}) and k_2 (g/mg/min) are the adsorption rate constants of pseudo-first-order and pseudo-second-order adsorption, respectively. The validity of the two models can be inspected from the linear plots of $\log(q_e - q_t)$ vs. t and (t/q_t) vs. t , respectively. The rate constants k_1 and k_2 can be obtained from the plot of experimental data (Zulfikar *et al.*, 2015).

All of the fitting parameters are presented in Table 3. Regarding the coefficient of determination (R^2), which indicates the goodness of fit, the pseudo-second-order model had it closer to 1 than the pseudo-first-order model. This indicates that the pseudo-second-order model provides a better fit to the experimental data, and effectively describes the adsorption process of IBP onto MMIPs based on the assumption of chemisorption of the adsorbate on the sorbent, where the adsorption rate is controlled by the adsorption mechanism (Mao *et al.*, 2016).

3.2.6 Thermodynamic studies

To evaluate the adsorption behavior of IBP onto MMIPs, the adsorption process was examined at the three temperatures 298 K, 313 K, and 333 K, with IBP 50 mg/L at pH 3 for 90 min. The estimates of thermodynamic parameters, including the Gibbs free energy change (ΔG°), enthalpy change (ΔH°), and entropy change (ΔS°), were determined based on experimental data using the following equations:

$$\Delta G^\circ = \Delta H^\circ - T\Delta S^\circ \quad (7)$$

$$\Delta G^\circ = -RT \ln K_d \quad (8)$$

where K_d is the thermodynamic distribution coefficient of the sorbent, R is the universal gas constant (8.314 J/mol K) and T (K) is the reaction temperature.

Thermodynamic parameters obtained from the IBP adsorption onto MMIPs at different temperatures are presented in Table 4. The negative Gibbs free energy change (ΔG°) indicates that the adsorption process occurs spontaneously. Meanwhile, it was also found that the value of ΔG° decreased with temperature, indicating that adsorption was favored at higher temperatures. The enthalpy change (ΔH°) is negative, which indicates that this adsorption is an exothermic process. Furthermore, the apparent ΔH of the binding of ibuprofen was below 40 kJ/mol indicating that the binding occurred through physisorption (Cantu *et al.*, 2015).

Table 3. Kinetic parameters for adsorption of IBP on MMIPs

$q_{e,exp}$	Pseudo-first-order			Pseudo-second-order		
	K_1 (min^{-1})	$q_{e,cal}$ (mg/g)	R^2	K_2 (g/mg min)	$q_{e,cal}$ (mg/g)	R^2
15.6760	0.0307	7.3770	0.8679	0.0071	16.5893	0.9982

Table 4. Thermodynamic parameters for adsorption of IBP on MMIPs

Temperature (K)	ΔG° (kJ/mol)	ΔH° (kJ/mol)	ΔS° (J/mol K)
298	-24.5396		
313	-24.6597	-22.1535	8.0072
333	-24.8199		

Besides, the ΔS° was positive, indicating an increase in randomness in the solid-solution interface. It may be related to the structure change of adsorbate or adsorbent.

4. Conclusions

Magnetic molecularly imprinted polymers (MMIPs) were synthesized using the bulk polymerization method and characterized by FT-IR, SEM-EDS, TEM, VSM and zeta potential analyzer. The optimal conditions for IBP removal by MMIPs were found to be pH 3, a contact time of 90 min, and an adsorbent mass of 25 mg. The adsorption isotherm study revealed that the adsorption of IBP onto MMIPs followed a monolayer adsorption mechanism on a homogeneous surface, as described by the Langmuir model. The kinetics study indicated that the adsorption process followed pseudo-second-order kinetics. The thermodynamic data showed that the adsorption on the surface of MMIPs was spontaneous and exothermic.

Acknowledgements

Research facility support for this work was provided by Bandung Institute of Technology, Faculty of Mathematics and Natural Sciences, Department of Chemistry.

References

- AL Falahi, O. A., Abdullah, S. R. S., Hasan, H. A., Othman, A. R., Ewadh, H. M., Al-Baldawi, I. A., . . . Ismail, N. I. (2021). Simultaneous removal of ibuprofen, organic material, and nutrients from domestic wastewater through a pilot-scale vertical sub-surface flow constructed wetland with aeration system. *Journal of Water Process Engineering*, 43(June), 102214. Retrieved from <https://doi.org/10.1016/j.jwpe.2021.102214>
- Cantu, Y., Remes, A., Reyna, A., Martinez, D., Villarreal, J., Trevino, S., . . . Parsons, J. G. (2015). Thermodynamics, kinetics, and Activation energy studies of the sorption of chromium (III) and chromium(VI) to a Mn3O4 nanomaterial. *Chemical Engineering Journal*, 254(956), 374–383. Retrieved from <https://doi.org/10.1016/j.cej.2014.05.110>. Thermodynamics

- Dai, C. M., Geissen, S. U., Zhang, Y. L., Zhang, Y. J., & Zhou, X. F. (2011). Selective removal of diclofenac from contaminated water using molecularly imprinted polymer microspheres. *Environmental Pollution*, 159(6), 1660–1666. Retrieved from <https://doi.org/10.1016/j.envpol.2011.02.041>
- Farré, M., Ferrer, I., Ginebreda, A., Figueras, M., Olivella, L., Tirapu, L., . . . Barceló, D. (2001). Determination of drugs in surface water and wastewater samples by liquid chromatography-mass spectrometry: Methods and preliminary results including toxicity studies with *Vibrio fischeri*. *Journal of Chromatography A*, 938(1–2), 187–197. Retrieved from [https://doi.org/10.1016/S0021-9673\(01\)01154-2](https://doi.org/10.1016/S0021-9673(01)01154-2)
- Fauziah, S., Soekanto, N. H., Budi, P., & Taba, P. (2019). Adsorption capacity and selectivity of molecularly imprinted polymer towards β -Sitosterol. *Asian Journal of Chemistry*, 31(11), 2527–2531.
- He, D., Zhang, X., Gao, B., Wang, L., Zhao, Q., Chen, H., . . . Zhao, C. (2014). Preparation of magnetic molecularly imprinted polymer for the extraction of melamine from milk followed by liquid chromatography-tandem mass spectrometry. *Food Control*, 36(1), 36–41. Retrieved from <https://doi.org/10.1016/j.foodcont.2013.07.044>
- Huang, W., Li, H., Xu, W., Zhou, W., Zhou, Z., & Yang, W. (2012). Selective adsorption of dibenzothiophene using magnetic molecularly imprinted polymers. *Adsorption Science and Technology*, 30(4), 331–343. Retrieved from <https://doi.org/10.1260/0263-6174.30.4.331>
- Husin, N. A., Muhamad, M., Yahaya, N., Miskam, M., Syazni Nik Mohamed Kamal, N. N., Asman, S., . . . Mohamad Zain, N. N. (2021). Application of a new choline-imidazole based deep eutectic solvents in hybrid magnetic molecularly imprinted polymer for efficient and selective removal of naproxen from aqueous samples. *Materials Chemistry and Physics*, 261(June 2020), 124228. Retrieved from <https://doi.org/10.1016/j.matchemphys.2021.124228>
- Lach, J., & Szymonik, A. (2020). Adsorption of diclofenac sodium from aqueous solutions on commercial activated carbons. *Desalination and Water Treatment*, 186(September 2019), 418–429. Retrieved from <https://doi.org/10.5004/dwt.2020.25567>
- Madikizela, L. M., & Chimuka, L. (2016). Synthesis, adsorption and selectivity studies of a polymer imprinted with naproxen, ibuprofen and diclofenac. *Journal of Environmental Chemical Engineering*, 4(4), 4029–4037. Retrieved from <https://doi.org/10.1016/j.jece.2016.09.012>
- Mao, Y., Cui, J., Zhao, J., Wu, Y., Wang, C., Lu, J., . . . Yan, Y. (2016). Selective separation of bifenthrin by pH-sensitive/magnetic molecularly imprinted polymers prepared by pickering emulsion polymerization. *Fibers and Polymers*, 17(10), 1531–1539. Retrieved from <https://doi.org/10.1007/s12221-016-6570-0>
- Moral-Rodríguez, A. I., Leyva-Ramos, R., Carrasco-Marín, F., Bautista-Toledo, M. I., & Pérez-Cadenas, A. F. (2020). Adsorption of diclofenac from aqueous solution onto carbon xerogels: Effect of synthesis conditions and presence of bacteria. *Water, Air, and Soil Pollution*, 231(1). Retrieved from <https://doi.org/10.1007/s11270-019-4385-5>
- Ningtyas, K. W., Zulfikar, & Piluharto, B. (2015). Identifikasi Ibuprofen, Ketoprofen dan Diklofenak Menggunakan Test Strip Berbasis Reagen Spesifik yang Diimobilisasi pada Membran Nata De Coco. *Jurnal Ilmu Dasar*, 16(2), 49–54.
- Oba, S. N., Ighalo, J. O., Aniagor, C. O., & Igwegbe, C. A. (2021). Removal of ibuprofen from aqueous media by adsorption: A comprehensive review. *Science of the Total Environment*, 780, 146608. Retrieved from <https://doi.org/10.1016/j.scitotenv.2021.146608>
- Olcer, Y. A., Demirkurt, M., Demir, M. M., & Eroglu, A. E. (2017). Development of molecularly imprinted polymers (MIPs) as a solid phase extraction (SPE) sorbent for the determination of ibuprofen in water. *RSC Advances*, 7(50), 31441–31447. Retrieved from <https://doi.org/10.1039/c7ra05254e>
- Rizki, A., Syahputra, E., Pandia, S., & Halimatusdahlia. (2019). Pengaruh Waktu Kontak dan Massa Adsorben Biji Asam Jawa (*Tamarindus indica*) dengan Aktivator H₃PO₄ terhadap Kapasitas Adsorpsi Zat Warna Methylene Blue. *Jurnal Teknik Kimia USU*, 8(2), 54–60. Retrieved from <https://doi.org/10.32734/jtk.v8i2.1881>
- Rizqi Utami, A., Ali Zulfikar, M., & Wahyuningrum, D. (2021). The synthesis of magnetic molecularly imprinted polymer against di-(2-ethylhexyl) phthalate. *IOP Conference Series: Materials Science and Engineering*, 1143(1), 012003. Retrieved from <https://doi.org/10.1088/1757-899x/1143/1/012003>
- Sahin, O. I., Saygi-Yalcin, B., & Saloglu, D. (2020). Adsorption of ibuprofen from wastewater using activated carbon and graphene oxide embedded chitosan-pva: Equilibrium, kinetics, and thermo dynamics and optimization with central composite design. *Desalination and Water Treatment*, 179, 396–417. Retrieved from <https://doi.org/10.5004/dwt.2020.25027>
- Samah, N. A., Sánchez-Martín, M. J., Sebastián, R. M., Valiente, M., & López-Mesas, M. (2018). Molecularly imprinted polymer for the removal of diclofenac from water: Synthesis and characterization. *Science of the Total Environment*, 631–632, 1534–1543. Retrieved from <https://doi.org/10.1016/j.scitotenv.2018.03.087>
- Uzuriaga-Sánchez, R. J., Wong, A., Khan, S., Pividori, M. I., Picasso, G., & Sotomayor, M. D. P. T. (2017). Synthesis of a new magnetic-MIP for the selective detection of 1-chloro-2, 4-dinitrobenzene, a highly allergenic compound. *Materials Science and Engineering C*, 74, 365–373. Retrieved from <https://doi.org/10.1016/j.msec.2016.12.019>
- Xia, Q., Yun, Y., Li, Q., Huang, Z., & Liang, Z. (2017). Preparation and characterization of monodisperse molecularly imprinted polymer microspheres by precipitation polymerization for kaempferol. *Designed Monomers and Polymers*, 20(1), 201–209. Retrieved from <https://doi.org/10.1080/15685551>

- 2016.1239174
- Yulianti, S., & Darvina, Y. (2020). Pengaruh komposisi CoFe₂O₄ terhadap sifat magnetik nanokomposit CoFe₂O₄/PVDF yang disintesis dengan metode solgel. *Pillar of Physics*, 13(April), 10–17.
- Zhang, J., Ma, C., Li, H., Wang, X., Ning, F., Kang, M., & Qiu, Z. (2021). Polyethyleneimine modified magnetic microcrystalline cellulose for effective removal of congo red: Adsorption properties and mechanisms. *Fibers and Polymers*, 22(6), 1580–1593. Retrieved from <https://doi.org/10.1007/s12221-021-0543-7>
- Zhi, K., Wang, L., Zhang, Y., Zhang, X., Zhang, L., Liu, L., . . . Xiang, W. (2018). Preparation and evaluation of molecularly imprinted polymer for selective recognition and adsorption of gossypol. *Journal of Molecular Recognition*, 31(3), 1–9. Retrieved from <https://doi.org/10.1002/jmr.2627>
- Zulfikar, M. A., Wahyuningrum, D., Mukti, R. R., & Setiyanto, H. (2015). Molecularly imprinted polymers (MIPs): A functional material for removal of humic acid from peat water. *1069218*, 1–12. Retrieved from <https://doi.org/10.1080/19443994.2015.1069218>